

High-Performance Chromium-Free Coatings for Electrical Steels

KANG-YUNG PENG*, KUO-CHU HSIEH, RUEG-MING CHEN***
and YU-PING SUI******

* *New Materials Research & Development Department*

** *Technology Planning & Development Department*

*** *Rolling Mill Department - III*

**** *Metallurgical Department*

China Steel Corporation

Electrical steels (ES) are the core material for power generators, compressors, electrical motors and transformers. Even though the chromium (Cr)-containing ES coatings are not environment-friendly, they are still dominant. Improvements in performance are required for the Cr-free ES coatings to compete with the mature Cr technologies. In this report, two of the next generation Cr-free ES coatings, C6NM and C6N8-G, are presented and evaluated. Compared with the standard Cr-free coating C6N8, both C6NM and C6N8-G have better corrosion resistance, interlayer electrical resistance, adhesion to substrates, and capability against cutting-edge rusting. C6NM not only shows comparable performance to the standard Cr-containing C628 coating but overwhelms it in the adhesion and insulation capability. The new coatings presented here, C6NM and C6N8-G, are expected to promote the application of environment-friendly Cr-free technologies in general-purpose applications as well as high-performance ES products.

Keywords: Electrical steel, Coating, Chromium-free, Insulation, Corrosion

1. INTRODUCTION

Electrical steels (ES), or silicon steels, are an important family of steels that consist of Fe-Si alloys. Such alloys have special electromagnetic properties and are the key components in modern electrical and mechanical systems such as wind generators, electrical motors, transformers, and compressors. Since these electrical and mechanical systems are used as the core where energy transforms (between forms of electricity and/or machine), their properties are very critical to the efficiency of the energy transformation.

The loss during the energy transformation (i.e., the “iron loss”) is composed of the hysteresis loss and the Eddy current loss⁽¹⁾. The former is an intrinsic property and is mainly controlled by the alloy composition and process history of the electrical steel. On the other hand, the latter depends more on extrinsic parameters, e.g., the design of the energy-transforming systems and the geometry of the ES core. Since Eddy current loss is proportional to the square of thickness, electrical steels are usually used in the form of a stacked pile of thin sheets. Moreover, Eddy current loss is also inversely proportional to the interlayer resistivity between the ES sheets. Therefore modern ES coils are always coated with an insulating layer^(2,3).

Since steels are liable to be corroded by humidity, air, salt, and other corrosion factors, insulating coatings must also provide the anti-corrosion capability so that the durability of ES cores can be guaranteed in the application.

Besides interlayer insulation and corrosion resistance, adhesion to substrate, capability of annealing, and punch workability are also required for the ES coatings to survive the processing conditions. However, it is difficult to develop high-performance coatings with good properties in all the required aspects. Therefore, ES coatings usually have application-oriented and compromised compositions.

There are two main categories of coatings for ES: the chromium (Cr)-containing systems; and the Cr-free systems. And so far Cr-containing coatings have been the standard coating for decades. However, Cr-containing coatings use hexavalent chromium Cr⁺⁶, which is a toxic carcinogen and has already been legally regulated^(4,5). Nevertheless, Cr-containing coatings are still the major category for ES coatings till now, due to their outstanding corrosion-inhibiting and self-healing capabilities⁽⁶⁾. Therefore Cr-free techniques that can perform as good as the Cr-containing coatings are in very high demand nowadays.

In this report, we disclose and investigate two of

the next-generation high-performance Cr-free ES coatings (C6NM and C6N8-G) that can compete with the traditional Cr-containing techniques in many aspects. These environment-friendly coatings can provide ES with excellent performance (interlayer resistivity, anti-corrosion properties, adhesion to substrates, annealing capability, and the anti-rust ability of cutting edges) to fulfill exceedingly well all the requirements for general-purpose applications as well as those for high-end products.

2. EXPERIMENTAL METHOD

The materials

The coatings under investigation are all from waterborne paints. C628 and C6N8 are the standards for Cr-containing and Cr-free coatings, respectively. C6N8-G and C6NM are the newly-developed Cr-free coatings that have improved performance. C6N8-G is similar in composition to the standard C6N8, but adopts a different organic system that is specifically designed for use in ES paints. A new set of organic binders and inorganic sinters is used in C6NM so that it has a fundamentally different recipe from C6N8 and C6N8-G. The ES substrate for the investigated samples is 50CS1300. All the samples are products that were coated nearby within a couple of days in the Electrical Steel Coating Line (ESCL) or the Continuous Coating Line (CCL), with an average coating thickness of $0.70 \pm 0.20 \mu\text{m}$. The samples are listed in Table 1. As a sulfur content of 0.005% is more representative for regular 50CS1300 substrates, coated coils from substrate lot #6U337 are investigated. However, to clarify the effect of coatings on the cutting-edge rusting, samples from a substrate with a higher sulfur content ($S=0.008\%$, substrate lot #6U250) are also evaluated in the atmosphere exposure test.

Cross-sectional images of the coatings

The samples were first vapor deposited by a thin layer of platinum (Pt). Then the surface was milled by

dual-beam focused gallium ion beams (DB-FIB) (FEI Nova-200 NanoLab Compatible, Center for Micro/Nano Science and Technology, National Cheng-Kung University) to cut out a rectangular hole, from which cross sectional images can then be taken by scanning electron microscopy (SEM) at a magnification of 65000X.

Anti-corrosion capability

The anti-corrosion capability of ES coatings was evaluated in a salt-spray tester (SST) on $8 \times 15 \text{ cm}^2$ edge-sealed samples. The salt spray was produced from 35°C 5% NaCl aqueous solution at a rate of 1~2 mL/hr. After exposure to the salt spray for a specified period of time (e.g., 5Hrs), samples were then judged by the area percentage of corrosion.

Electrochemical analysis

The coated and bare 50CS1300 ES samples were tested in a fresh 3.5% NaCl aqueous solution by an electrochemical analyzer (ACM Field Machine). Pt and Ag/AgCl-3M KCl are used as the counter and the reference electrodes, respectively. The sample (as the working electrode) was tested on an area of 1 cm^2 exposed to the salt solution. The coated samples were tested without pre-cleaning but a small part of coatings outside the tested area was polished off for the electrical connection. The whole experiment set-up was first left open-circuited for a 15 min stabilization period before the measurement. However, the bare substrate was tested immediately after being thoroughly cleaned by detergent and de-ionized water. For each potentiodynamic test, the rest potential of system (E_R) was determined and a scan for polarization curve was then carried out from ca -250 to 600 mV (versus E_R) at a scan rate of 1 mV/s⁽⁷⁾.

Interlayer resistivity

The insulation capability of the ES coatings was evaluated by the “interlayer resistivity R_s ” (in $\Omega \text{cm}^2/\text{sheet}$) of $10 \times 30 \text{ cm}^2$ samples on a JIS-C-2550 verified interlaminar resistivity tester. A typical test

Table 1 Samples for different coatings in the investigation

50CS1300 coated ES products			
Coating		Substrate	Source
Name	Type	lot # 6U337 (S = 0.005%)	lot # 6U250 (S = 0.008%)
C628	Standard Cr-containing	Coil #1747083	Coil #1746131 CCL
C6N8	Standard Cr-free	Coil #1747082	Coil #1746133 ESCL
C6N8-G	Newly-developed Cr-free	Coil #1747049	Coil #1746127 ESCL
C6NM	Newly-developed Cr-free	Coil #1747080	Coil #1746128 ESCL

was to measure the current **I** (in Amp) passing across the coating from the ES substrate to the electrode pads that are pressed to the coating. The interlayer resistivity was calculated from the measured current **I** and the total contact area of the electrode pads **A** (in cm². A is 10 for the instrument used.) by the Equation below. For ordinary ES applications, an interlayer resistivity of 10 Ω·cm²/sheet is quite sufficient. For high-efficiency products where the Eddy current loss needs to be reduced as low as possible, a higher value (e.g., 50Ω·cm²/sheet) is required.

$$R_s = A \left[\frac{1}{I} - 1 \right]$$

Adhesion

The adhesion of coating to ES substrate was evaluated by an immersion test (5% CuSO_{4(aq)}) solution for a specified period of time, e.g., 10 sec) on the bent (6, 4, and 2 mm in diameter) and impacted (by a 500g rod with a hemisphere of 12.5mm in diameter at end falling freely from a height of 50cm) 5×8cm² samples. If the coating does not adhere sufficiently to the substrate, bending and impact will result in delamination of coating and cracks, where red rust shows up due to a spontaneous redox reaction between Fe and Cu⁺². The adhesion capability of coatings to substrate can be differentiated easily by the extent of corrosion after the immersion.

Stress-relieving annealing (SRA) capability

A standard stress-relieving annealing condition for ES at 750°C for one hour in nitrogen atmosphere was used. The heating rate was less than 200°C per hour. The capability of annealing for ES coatings was then evaluated by the Scotch tape (type 600) adhesion test. Annealed samples that show no peeling and no powdering are verified to be capable of SRA.

Anti-rust capability of cutting edges

The coated ES coils were punched into 30mm × 60mm size. For each sample, 50 pieces were then compactly stacked by a tape to a pile of 25mm height. One surface of the cutting edges was oiled with S-162N punch oil (Peisun Chemical Co., Ltd.) while other surfaces were left bare. The 8 piles (4 coatings × 2 substrates) of punched ES were then exposed in-doors to the ambient atmosphere in the same environment and for the same period of time. The anti-rust capability of the cutting edges for each coating was then evaluated by the extent of corrosion on the cutting edges at days 7, 17, 29 and 109.

3. RESULTS AND DISCUSSION

The anti-corrosion capability of coatings

The cross sectional images of C628, C6N8, C6N8-G and C6NM coatings are shown in Fig.1. For all the images, it is the middle porous layer that presents the cross section of the coating. The top dense layer is the protecting Pt film deposited prior to DB-FIB milling. And the bottom dense layer is the ES substrate. Due to the rapid loss of water during the baking and curing of the paints, all coatings show porosity to some extent. The pores in C628 are tiny, circular, and uniformly dispersed in the coating. Such pores are too small to form a continuous cave network. On the contrary, the pores in C6N8 and C6N8-G are bigger and more irregular, suggesting the presence of empty tunnels in the coating. For C6NM, a lower extent of porosity and a relatively more compact structure can be observed.

From Figure 1, C6NM and C628 can be expected to have the best barrier capability against corrosion factors. As shown in Figure 2, the results of the salt spray test (SST) support this deduction. After SST, C6NM shows no corrosion and C628 has only traces of rust. In contrast, C6N8 has been about 50% corroded. The most distinctive feature in Figure 2 is that C6N8-G is much better than C6N8 for the presented SST results, even though Figure 1 indicates a similar extent of porosity for both. The marked difference between C6N8-G and C6N8 in the SST result is due to different organic systems being used in the two paints. C6N8 contains a high content of hydrophilic emulsifiers by which the humidity resistance of the coating is somewhat affected. However, a reactive organic system is adopted in C6N8-G so that the coating can be rendered relatively more hydrophobic after curing.

The results of potentiodynamic scans on the coated ES and the bare 50CS1300 substrate are shown in Fig.3 (all the potentials are presented versus the reference Ag/AgCl-3MKCl). The bare ES substrate has a rest potential (E_R) of -710mV. The Cr-free coatings C6N8, C6N8-G and C6NM have E_R at -597, -614, and -596 mV, respectively. The positive shifts in the E_R of coated samples from that of bare substrate reveal the capability of the coatings to thermodynamically hamper the corrosion of the ES substrate in the salt solution. The Cr-containing C628 coating has the most positive shift in E_R (-710 to -564mV), revealing that it has the most powerful inhibiting effect against corrosion among the investigated coatings.

By extrapolating the cathodic branch of the polarization curve to E_R the corrosion current density can be obtained to calculate the theoretic corrosion rate and relative anti-corrosion efficiency for each sample. The results are listed in Table 2. The corrosion current density of the bare 50CS1300 ES substrate is 17.5

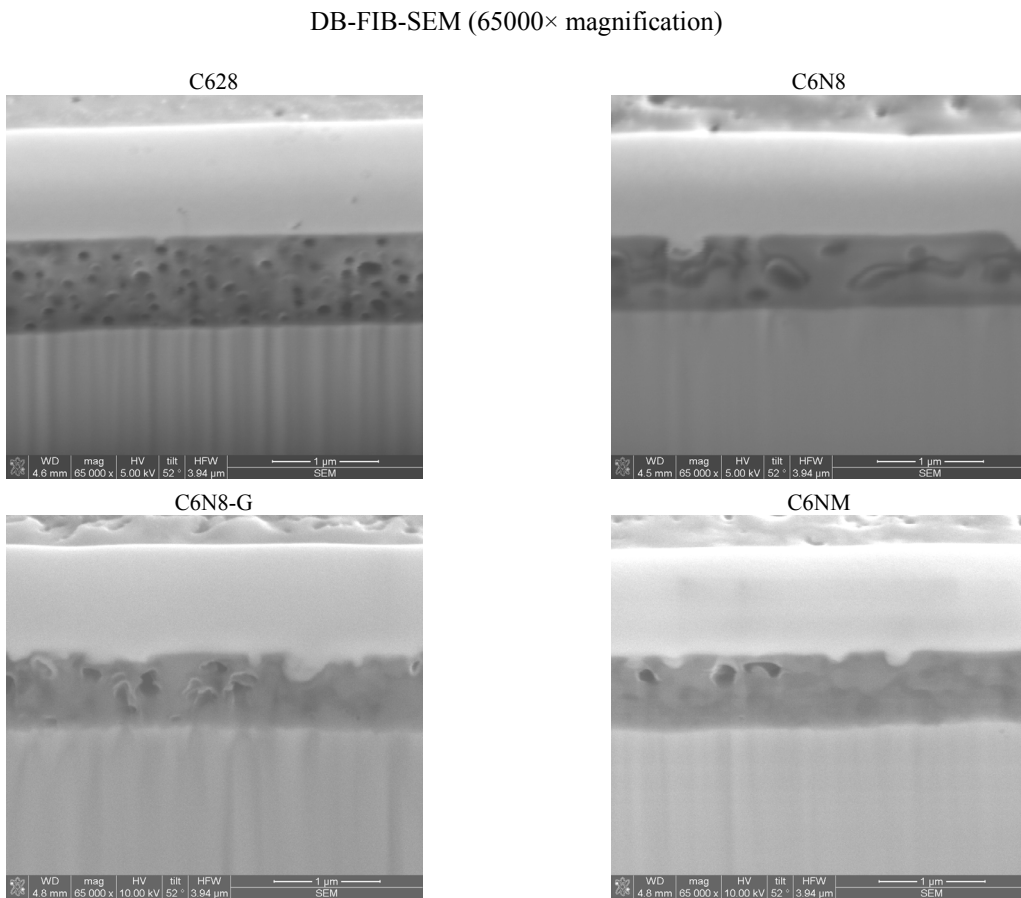


Fig.1. The cross sectional SEM images (65000 \times) for ES (50CS1300) with different coatings: C628, C6N8, C6N8-G and C6NM.

Table 2 Corrosion current density and the corresponding corrosion rate for the investigated coated ES and bare ES substrate (extracted from Figure 3)

	Coated ES				Bare ES
	C628	C6N8	C6N8-G	C6NM	50CS1300
Corrosion current density ($\mu\text{A}/\text{cm}^2$)	1.10	2.70	1.40	0.70	17.50
Corrosion rate(mils/year)*	0.53	1.29	0.67	0.33	8.37
Anti-corrosion efficiency (%)**	93.7	84.6	92.0	96.1	defined as 0

* For iron, corrosion rate (mils/year) = $0.4782 \times$ corrosion current density ($\mu\text{A}/\text{cm}^2$)

** Anti-corrosion efficiency = $[1 - \text{Corrosion rate}_{\text{Coating}} / \text{Corrosion rate}_{\text{Bare}}] \times 100\%$

$\mu\text{A}/\text{cm}^2$, slightly smaller than that of iron in 3.5% NaCl solution ($25.0 \mu\text{A}/\text{cm}^2$)⁽⁸⁾. The standard Cr-containing C628 coating has a smaller corrosion current density ($1.10 \mu\text{A}/\text{cm}^2$) than the standard Cr-free C6N8 coating ($2.70 \mu\text{A}/\text{cm}^2$). This accords with the common conception: Cr-containing coatings usually have stronger anti-corrosion capabilities. However, as can be seen in Table 2, both the newly-developed Cr-free coatings

C6N8-G and C6NM have better anti-corrosion capabilities (smaller corrosion current density: 1.40 and $0.70 \mu\text{A}/\text{cm}^2$) than the standard Cr-free C6N8 coating. Moreover, these two new Cr-free coatings are either close to or even better than C628. This reveals that corrosion can be suppressed as significantly in the Cr-free C6N8-G and C6NM coatings as in the Cr-containing C628. This conclusion is fully consistent with the SST results in Fig.2.

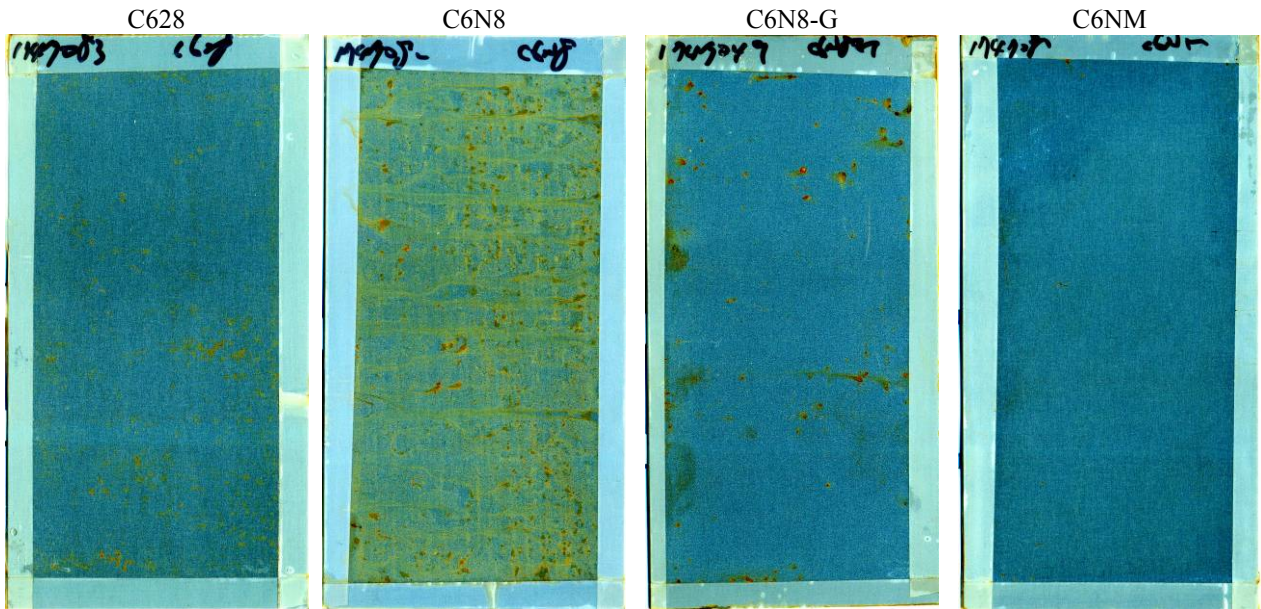


Fig.2. 5Hrs salt spray test results for ES (50CS1300) with different coatings: C628, C6N8, C6N8-G, and C6NM.

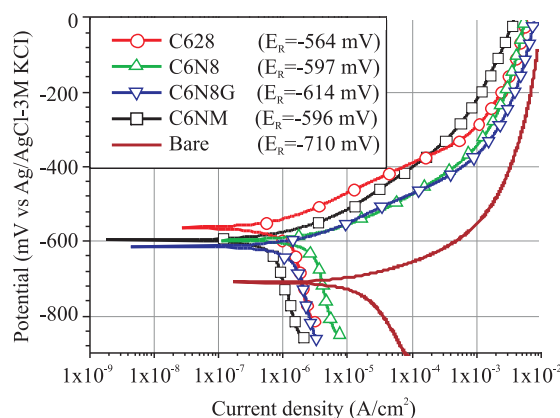


Fig.3. Polarization curves for ES (50CS1300) with different coatings (C628, C6N8, C6N8-G, C6NM) and as bare substrate.

The interlayer resistance of coatings

The electrical insulating property of coatings is one of the key parameters that determine the efficiency of energy transformation in ES systems. As described in the Experimental Method, a high interlayer resistance is required to reduce the iron loss. Table 3 shows typical interlayer resistivity (R_s) values for ES with the investigated coatings (thickness: $0.70\pm0.20\ \mu\text{m}$). For the standard coatings C628 and C6N8, interlayer insulation of $6\sim40\ \Omega\text{cm}^2/\text{sheet}$ can be attained. Compared with C6N8, the newly-developed C6N8-G Cr-free coating is less hydrophilic so that the interlayer

resistivity of C6N8-G is higher ($10\sim60\ \Omega\text{cm}^2/\text{sheet}$). For the C6NM Cr-free coating, it contains inorganic sinters so that a strong electrical insulation of $30\sim150\ \Omega\text{cm}^2/\text{sheet}$ can be realized.

Table 3 Interlayer resistivity R_s of the investigated coatings (thickness: $0.70\pm0.20\ \mu\text{m}$)

Interlayer resistivity R_s ($\Omega\text{cm}^2/\text{sheet}$)			
C628	C6N8	C6N8-G	C6NM
6~40	6~40	10~60	30~150

The adhesion of coatings to ES substrates

For application, ES must be worked into appropriate dimensions such as strips, rings, hemi-circles, and E and I shapes. Working processes like slitting, punching and stacking could locally deform substrates, leave stress, and finally damage the coating. Moreover, the materials can fall off in the working processes from damaged coatings to cause problems such as powder accumulation, contamination-induced rust, damage to punch dies, and additional maintenance of equipments. Therefore, the adhesion capability of coating to substrate is important to the workability of ES.

The impact and bending tests described in the Experimental Method are adopted to evaluate the adhesion capability for the investigated coatings and the results are summarized in Tables 4 and 5. For convenience, a ranking value is given for each test and the

Table 4 Impact (concave and convex) test results on ES (50CS1300) with different coatings (Best 5 → Worst 1)

	Impact test			
	C628	C6N8	C6N8-G	C6NM
Photo				
Ranking	Concave 2.0	2.0	3.0	3.5
	Convex 2.0	2.0	2.5	3.5

Table 5 Bending test results on ES (50CS1300) with different coatings at the diameter of: (a) 6mm, (b) 4mm, and (c) 2mm (Best 5 → Worst 1)

	Bending test			
	(a) $\phi = 6\text{mm}$	(b) $\phi = 4\text{mm}$	(c) $\phi = 2\text{mm}$	
Photo	C628 C6N8 C6N8-G C6NM 			
Ranking	C628 1.5	1.0	1.0	
	C6N8 2.0	1.5	1.0	
	C6N8-G 2.5	2.0	1.0	
	C6NM 4.0	3.0	2.5	

higher the value the better the adhesion. For the impact tests, the standard coatings C628 and C6N8 are both ranked as 2.0. For the bending tests at a diameter of 6mm and rusted by 5% $\text{CuSO}_4(\text{aq})$ for 10 seconds, the ranking is 1.5 for C628 and 2.0 for C6N8, respectively. For the same tests, the newly-developed Cr-free coatings C6NM and C6N8-G have a lesser extent of corrosion and are therefore ranked with higher values,

revealing the better adhesion of the coatings to substrate. It is worth noting that among the investigated coatings C6NM has the best adhesion capability to substrate. Even in the most extreme condition (e.g., bending at $\phi = 2\text{mm}$), the damage to C6NM coating is still very limited, while the bent area with the other coatings are totally rusted.

Stress-relieving annealing (SRA) capability

Figure 4 shows the adhesion capability of the investigated coatings after annealing ($750^{\circ}\text{C} \times 1$ hour in N_2) to the 50CS1300 ES substrate. After annealing, the original silver shining tone is lost and all the coatings turn to have a charcoal black appearance due to the carbonization of organic components. However, no powdering or peeling can be observed in the Scotch tape test for any of the annealed samples, revealing that all the investigated coatings can adhere tightly to substrate after annealing. (The non-uniformity in the photographs of the tapes in Figure 4 is due to reflections of the roof fluorescent tubes.) It is also worth noting that the inorganic sinners in C6NM can strengthen the annealing capability of the coating, making the annealing process more feasible to all grades of ES substances (not shown here).

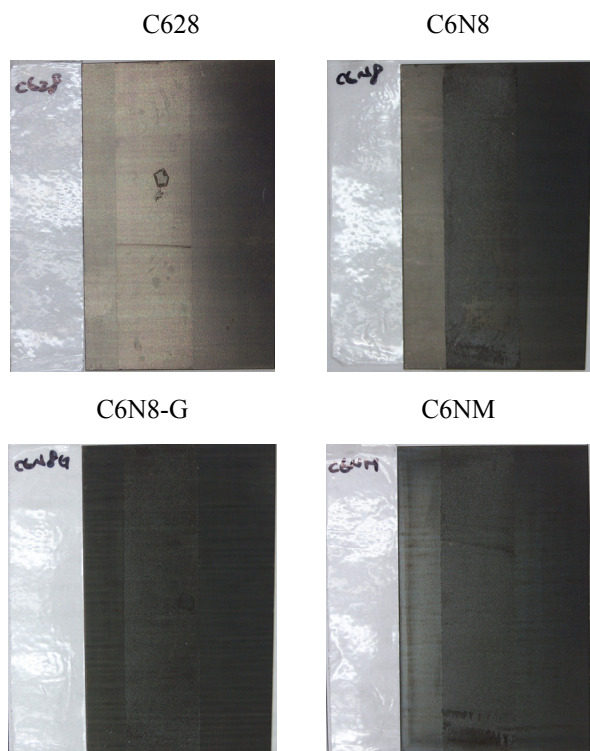


Fig.4. Scotch tape test results on the annealed ES (50CS1300) with the investigated coatings. For each photo, the left is the peeled Scotch tape and the right is the annealed sample with tape peeled.

The anti-rust capability of coatings on cutting edges

The working processes on ES such as slitting and punching create new cutting-edges where the substrate

is exposed to the atmosphere without the protection of a coating. Since post coating specifically on the cutting edges is not practically feasible, in most cases the cutting edges are just left as they were without any further treatment. Therefore, the rust usually shows up, if it ultimately does, first on the cutting edges of the worked ES pieces.

For the investigated coatings, rusting on the cutting edges of punched ES was compared by the indoor exposure of stacks of punched ES pieces to the atmosphere. Figures 5(a) shows the results for bare cutting edges of the ES with regular sulfur content (0.005%). Cutting-edge rust can be seen in Day 7 for all the coatings and but until Day 29 the extent of corrosion is still not severe. After a prolong exposure, rusting is obvious in Day 109 for all of the Cr-free coatings (C6N8, C6N8-G, and C6NM), while the cutting-edge rust is still very limited for the Cr-containing C628 coating.

Figure 5(b) shows the results for bare cutting edges of the ES with high sulfur content (0.008%). The cutting-edge rust does not show up in the first week of exposure for any of the samples. For the Cr-free coatings (C6N8, C6N8-G and C6NM), rusting begins on the bare cutting edges in the second week of exposure and then proceeds smoothly. For the stack with Cr-containing C628 coating, corrosion on the bare cutting edges is also observed in Day 17; however, little augmentation can be seen even after exposure for 109 days.

In practice, ES sheets must be processed using some kind of assisting lubricant. For example, punch oil is always used in the punching process of ES to guarantee the durability of dies. To clarify the effect of coating on the cutting-edge rusting in the presence of punch oil, for each stack of ES one surface of the cutting edges was also oiled by a commercial ES punch oil. Figure 5(c) shows the atmosphere exposure results for the oiled cutting edges of the ES with regular sulfur content (0.005%). Compared with the bare edges (Figure 5(a)), rusting proceeds faster on all the oiled edges in the first week. We attribute the accelerated initial-edge rusting on the oiled edges to the content of Cl (~500ppm) and S (~200ppm) in the punch oil. However, by Day 109, the cutting-edge rust for all the samples has only increased to a very limited extent, revealing the suppressing effect of this punch oil on the edge rusting during prolonged exposure. Figure 5(d) shows the results for oiled cutting edges of the ES with a high sulfur content (0.008%). Compared with Figure 5(b), the initial acceleration and long-term suppression on rusting for oiled cutting edges can also be observed in the ES with a high sulfur content (0.008%).

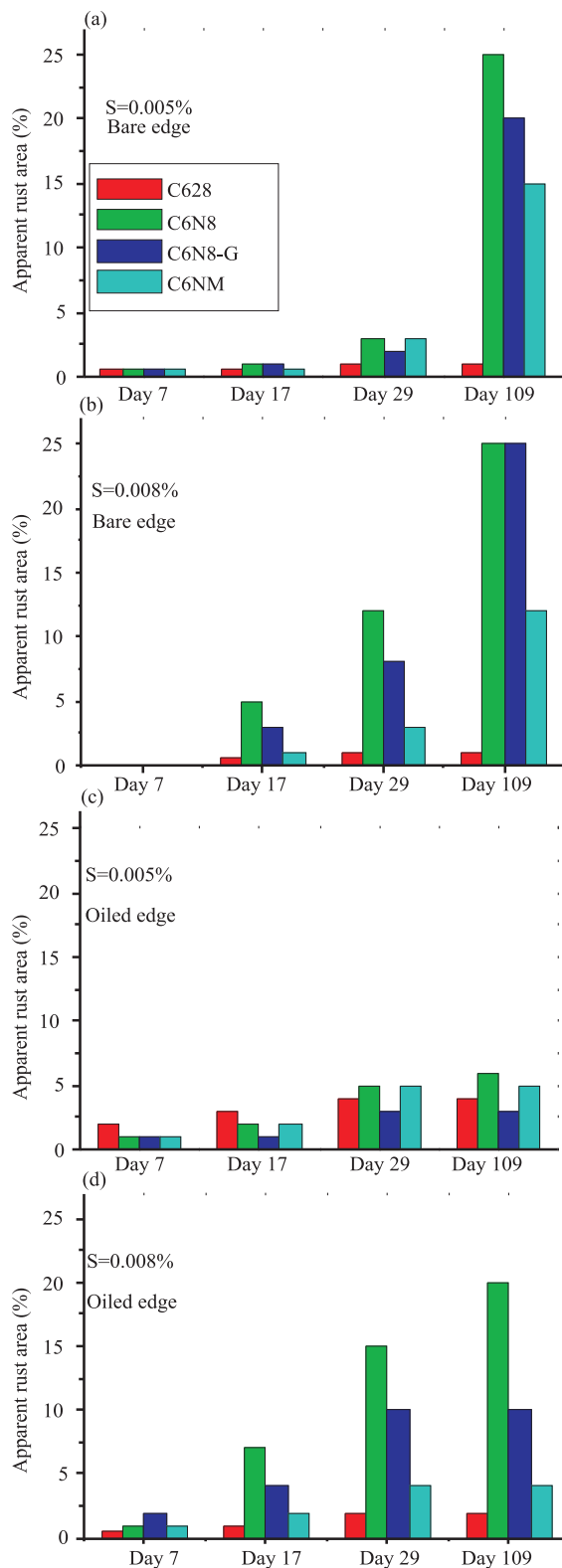


Fig.5. Atmosphere exposure test to evaluate the anti-rust capability of the coatings on cutting edges of ES (50CS1300): (a) bare, substrate sulfur content = 0.005%, (b) bare, substrate sulfur content = 0.008%, (c) with punch oil, substrate sulfur content = 0.005%, (d) with punch oil, substrate sulfur content = 0.008%.

From Figure 5, the best coating for protection against cutting-edge rusting is the Cr-containing C628. Since C628 has an only moderate capability of adhesion to substrate, the punching process unavoidably causes some particles of the coating materials to fall onto the surface of the cutting edges. We believe that it should be the self-healing ability of these particles that imparts the anti-rust capability to the cutting edges of C628-coated ES. For the Cr-free coating C6N8, however, no such self-healing capability exists. Thus, instead of preventing rusting, particles falling on the surface of the cutting edges introduce local electrochemical reactions around the contaminated sites in which corrosion starts. This should be the reason why C6N8 can not compete with C628 in the capability against cutting-edge rusting in Figures 5(a), (b) and (d). However, it is also worth noting that as long as the ES substrate has a low sulfur content and the cutting edges are properly oiled (Figure 5(c)), rusting on the surface of cutting edges can be controlled comparably both for the Cr-containing C628 and the Cr-free C6N8 coatings.

It should be emphasized that, as shown in Figure 5, both of the newly-developed Cr-free coatings C6N8-G and C6NM are again better than C6N8, in their capability against cutting-edge rusting. And among the investigated Cr-free coatings, C6NM is again the best in this aspect. Figures 5(c) and 5(d) reveal that C6NM can perform comparably to the Cr-containing C628 coating in practical conditions (i.e., when punch oil is used). Figure 6 shows the photos taken on Day 109 for the oiled cutting edges of ES (sulfur content = 0.008%) in Figure 5(d). The competitiveness of C6NM to C628 in the anti-cutting-edge-rust capability is clearly demonstrated.

C628



C6N8



C6N8-G



C6NM

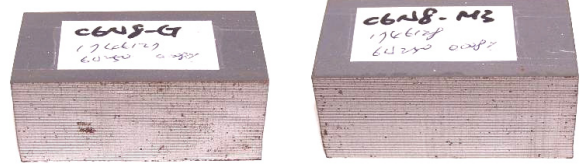


Fig.6. The appearance of S-162N punch oil-covered cutting edges of ES (50CS1300, substrate sulfur content = 0.008%) with different coatings after 109 days atmosphere exposure (the photo for Day 109 in Figure 5(d)).

4. CONCLUSIONS

In this report, two of our newly-developed Cr-free coatings, C6NM and C6N8-G, are exhibited. In comparison with the standard Cr-free C6N8 coatings, both C6NM and C6N8-G have better coating performance in the anti-corrosion property, adhesion to ES substrate, and the anti-rust capability on cutting edges. The newly-developed Cr-free coatings, C6NM and C6N8-G, can not only perform exceedingly well for general-purpose products, but also can fulfill the critical requirements for high-performance applications. Among the four investigated coatings (C628, C6N8, C6N8-G, and C6NM), C6NM is the best in the insulation, anti-corrosion, and adhesion capability, while in other aspects it can also compete with the standard Cr-containing C628 coating. We expect that the inventions presented here can further promote the application of environment-friendly Cr-free coatings in ES products.

REFERENCES

1. F.G Hanejko, G.W. Ellis, T.J. Hale: "Application of High Performance Material Processing -Electromagnetic Products" in PM2TEC'98 International Conference on Powder Metallurgy and Particulate Materials, Las Vegas, USA, May 31 – June 4, 1998.
2. M. Lindenmo, A. Coombs, D. Snell: J. Magn. Magn. Mater., 2000, vol. 215-216, pp. 79-82.
3. ASTM A 976:03 Standard Classification of Insulating Coatings by Composition, Relative Insulating Ability and Application.
4. Directive 2002/95/EC of The European Parliament and of The Council of 27 January 2003 on The Restriction of the Use of Certain Hazardous Substances in Electrical and Electronic Equipment (RoHS).
5. Directive 2002/96/EC of The European Parliament and of The Council of 27 January 2003 on Waste Electrical and Electronic Equipment (WEEE).
6. M. Kendig, S. Jeanjaquet, R. Addison, J. Waldrop: Surf. Coat. Tech., 2001, vol. 140, pp. 58-66.
7. G. Cabrera, F. Torres, J.C. Caicedo, W. Aperador, C. Amaya, and P. Prieto: J. Mater. Eng. Perform., 2010, vol. 21, pp. 128-136.
8. E. McCafferty: Corros. Sci., 2005, vol. 47, pp. 3202-3215. □